Available online at www.sciencedirect.com
SCIENCE DIRECT®
Journal of Organometallic Chemistry 680 (2003) 66–80
Journal of Organometallic Chemistry
www.elsevier.com/locate/jorganchem

Reactions of *nido*-1,2-$(Cp^*RuH)_2B_3H_7$ with RC≡CR′ (R, R′ = H, Ph; Me, Me) to yield novel metallacarboranes

Hong Yan, Alicia M. Beatty, Thomas P. Fehlner *

Department of Chemistry and Biochemistry, University of Notre Dame, 251 Nieuwland Science Hall, Notre Dame, IN 46556-5670, USA

Received 13 January 2003; received in revised form 14 March 2003; accepted 19 March 2003

Dedicated to Professor Fred Hawthorne on the occasion of his 75th birthday in honor of his pioneering research in carborane and metallacarborane chemistry.

Abstract

Addition of the internal alkyne, 2-butyne, to *nido*-1,2-$(Cp^*RuH)_2B_3H_7$ (**1**) at ambient temperature produces *nido*-1,2-$(Cp^*Ru)_2(\mu\text{-}H)(\mu\text{-}BH_2)$-4,5-$Me_2$-4,5-$C_2B_2H_4$ (**2**), *nido*-1,2-$(Cp^*RuH)_2$-4,5-Me_2-4,5-$C_2B_2H_4$ (**3**), and *nido*-1,2-$(Cp^*RuH)_2$-4-Et-4,5-$C_2B_2H_5$ (**4**), in parallel paths. On heating, **2**, which contains a novel *exo*-polyhedral borane ligand, is converted into *closo*-1,2-$(Cp^*RuH)_2$-4,5-Me_2-4,5-$C_2B_3H_3$ (**5**) and *nido*-1,6-$(Cp^*Ru)_2$-4,5-Me_2-4,5-$C_2B_2H_6$ (**6**) the latter being a framework isomer of **3**. Heating **2** with 2-butyne generates *nido*-1,2-$(Cp^*RuH)_2$-3-{CMeCMeB(CMeCHMe)$_2$}-4,5-Me_2-4,5-$C_2B_2H_3$ (**7**) in which the *exo*-polyhedral borane is triply hydroborated to generate a boron bound –CMeCMeB(CMeCHMe)$_2$ cluster substituent. Along with **3**, **4**, **5**, **6**, and **7**, the reaction of **1** with 2-butyne at 85 °C gives *closo*-1,7-$(Cp^*Ru)_2$-2,3,4,5-Me_4-6-$(CHMeCH_2Me)$-2,3,4,5-C_4B (**8**). Reaction of **1** with the terminal alkyne, phenylacetylene, at ambient temperature permits the isolation of *nido*-1,2-$(Cp^*Ru)_2(\mu\text{-}H)(\mu\text{-}CHCH_2Ph)B_3H_6$ (**9**) and *nido*-1,2-$(Cp^*Ru)_2(\mu\text{-}H)(\mu\text{-}BH_2)$-3-$(CH_2)_2$Ph-4-Ph-4,5-$C_2B_2H_4$ (**11**). The former contains a Ru–B edge-bridging alkylidene fragment generated by hydrometallation on the cluster framework whereas the latter contains an *exo*-polyhedral borane like that of **2**. Thermolysis of **11** results in loss of hydrogen and the formation of *closo*-1,2-$(Cp^*RuH)_2$-3-$(CH_2)_2$Ph-4-Ph-4,5-$C_2B_3H_3$ (**12**).

Keywords: Boron; Metallaboranes; Metallacarboranes; Alkynes; Cluster

1. Introduction

An efficient and high-yield route to metallaboranes based on the reaction of monocyclopentadienylmetal halides (Group 5–9) with monoboranes provides convenient access to metallaboranes [1,2]. The availability of this route creates the possibility of investigating the systematic reaction chemistry of hybrid transition metal–borane complexes. In an effort to access the broad trends in reactivity for diruthenapentaborane, our group and the Shimoi group have examined unimolecular elimination reactions, and bimolecular reactions with a variety of metal fragments, monoboranes and Lewis bases [3–8]. As a result, our understanding of how metal and borane fragment properties are expressed in overall reactivity continues to improve.

The structural and reaction chemistry of metallaboranes is a hybrid of transition metal complexes and boranes [9–13]. Given the reactivity of alkynes with transition metal complexes to yield carbyne complexes [14,15] and with boranes to yield carboranes [16], the reactivity of metallaboranes with alkynes provides a chemical platform to explore metal–borane competition for an alkyne. Metallacarboranes are reasonable products [17]. In addition, they are of considerable interest, e.g. catalytic applications are known [18] and the formation of B–C bonds within the coordination sphere of a metal provides a novel method for the functionalization of saturated hydrocarbons [19,20]. The pioneering work on the reaction of metallaboranes with alkynes to yield metallacarboranes was carried out in Grimes'

* Corresponding author. Tel.: +1-574-631-7234; fax: +1-574-631-6652.
E-mail address: fehlner.1@nd.edu (T.P. Fehlner).

0022-328X/03/$ - see front matter © 2003 Elsevier Science B.V. All rights reserved.
doi:10.1016/S0022-328X(03)00172-4

laboratory where it was demonstrated that the reaction of stable *nido*-2-$CpCoB_4H_8$, $Cp = \eta^5$-C_5H_5, with acetylene gave *nido*-1,2,3-$CpCoC_2B_3H_7$ synthesized earlier from a carborane and metal fragment source [21,22]. However, only a few studies followed this early work [23–25]. There are two main reasons: (1) the high barrier for the addition of an alkyne to a stable metallaborane requires vigorous reaction conditions (175 °C at 20 h in the example above) and leads to low yields of thermodynamically stable products; and (2) metallaborane reactants were only available in small quantities. Consequently, this route offered no advantages over the existing borane to carborane to metallacarborane route.

Recently, we reported the reactivity of isoelectronic *nido*-rhodaboranes and *nido*-ruthenaboranes toward alkynes and demonstrated that the rhodaborane promotes catalytic alkyne cyclotrimerization [26] whereas the ruthenaborane favors alkyne insertion [27,28]. In the present paper we report the novel chemistry generated from the reaction of *nido*-1,2-$(Cp^*RuH)_2B_3H_7$ with MeC≡CMe or PhC≡CH. When reaction barriers are lowered, not only are yields of known compound types higher but also examples of compounds with unprecedented structural features are generated. Hence, under kinetic control the borane to metallaborane to metallacarborane route possesses distinct advantages over the historical route to metallacarboranes.

2. Results and discussion

In contrast to *nido*-2-$CpCoB_4H_8$, *nido*-1,2-$(Cp^*RuH)_2B_3H_7$ (**1**), contains two "extra" *endo*-cluster hydrogen atoms required for the compound to meet the *nido* electron count prescribed by the cluster electron counting rules [29,30]. These hydrogens constitute a source of reactivity for **1** not present in the analogous cobalt compound. The resulting mild reaction conditions permit greater control of its reactivity with alkynes thereby permitting the observation of intermediates and the isolation of novel metallacarboranes.

2.1. *nido*-1,2-$(Cp^*Ru)_2(\mu$-$H)(\mu$-$BH_2)$-4,5-Me_2-4,5-$C_2B_2H_4$ (**2**)

Reaction of *nido*-1,2-$(Cp^*RuH)_2B_3H_7$ (**1**) with 2-butyne at ambient temperature yields one major product. Keep in mind that *nido*-1,2-$(Cp^*RuH)_2B_4H_8$ is always a minor byproduct of this reaction. The molecular mass and the electron counting rules suggest a *nido* seven atom cluster structure. However, the NMR data are not consistent with such a structure. In particular, the ^{11}B-NMR spectrum shows three chemically distinct boron atoms, one of which is associated with two terminal hydrogen atoms. But the proton NMR shows only three distinct BH_t resonances rather than four. Further the presence of one B–H–B, two inequivalent B–H–Ru and one Ru–H–Ru proton resonances adds to the mystery. Consistent with the proton spectrum, the ^{13}C-NMR spectrum shows two types of Cp* methyl resonances and two types of methyl group resonances. In addition, two very broad signals in the olefinic region can be associated with carbon atoms incorporated into the borane network. No known structure was reasonable and it took a solid state structure determination to solve the dilemma.

Compound **2** is, in fact, a *nido* six-framework-atom cluster with a pentagonal pyramidal shape (Fig. 1). The metal atoms are in apical and basal positions and the five-membered ring is symmetrical with the boron atoms adjacent to the basal ruthenium atom. The core cluster of **2** is the same as that found for eight skeletal electron pair (sep) [29,30] *nido*-1,2-$(Cp^*Ru)_2(\mu$-$H)_2$-4-C(O)OMe-4,5-$C_2B_2H_5$ observed earlier in the reaction of **1** with activated alkynes [26]. The "extra" boron atom of **2** is *exo*-polyhedral in the form of a BH_2 fragment that bridges one of the two Ru(apical)–B(basal) edges. Curiously, the framework boron atom to which the bridge is attached has no terminal hydrogen. Rather it is connected to the BH_2 fragment by a B–H–B bridge. If the *exo*-cluster BH_2 fragment is reasonably treated as a one electron ligand, then **2** also possesses the eight sep appropriate for its structure.

Although this structural feature is unprecedented, the existence of *exo*-polyhedral fragments in cluster systems is well known. Indeed, the *exo*-cluster BH_2 fragment in **2** is related to a terminal BH_2PR_3 fragment observed in a metallaborane [31], a BH_3 fragment bridging a B–B edge in a ferraborane [32], a BX fragment bridging a M–M edge in a dinuclear complex [33], and a metallaborane

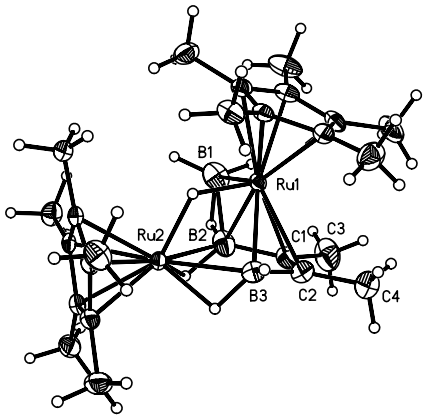

Fig. 1. Molecular structure (50% thermal ellipsoids) of *nido*-1,2-$(Cp^*Ru)_2(\mu$-$H)(\mu$-$BH_2)$-4,5-Me_2-4,5-$C_2B_2H_4$ (**2**). Selected bond lengths (Å) and angles (°): Ru(1)–B(2) 2.155(5), Ru(1)–B(1) 2.278(6), Ru(1)–B(3) 2.332(5), Ru(1)–C(1) 2.242(4), Ru(1)–C(2) 2.292(5), Ru(1)–Ru(2) 2.9134(5), Ru(2)–B(2) 2.293(6), Ru(2)–B(3) 2.327(6), B(1)–B(2) 1.760(9), C(1)–C(2) 1.391(8), C(1)–C(3) 1.508(7), C(2)–C(4) 1.519(7), C(1)–B(2) 1.558(7), C(2)–B(3) 1.520(8), C(2)–B(3)–Ru(2) 116.4(4), C(1)–B(2)–Ru(2) 118.8(4).

with an *exo*-polyhedral metal fragment [34]. Further, this structural feature is a direct analog of the product of the protonation of a dimetal complex bridged by a CH_2 fragment, which contains an agnostic C–H–M interaction, i.e. $Fe–CH_2–H–Fe^+$ [35].

In terms of stoichiometry, **2** forms from the reaction of **1** with a single alkyne. We have demonstrated earlier in a study of the reaction of CO with $(Cp^*Re)_2(\mu\text{-}H)_4B_4H_4$ that the addition of the Lewis base to a metal atom is accompanied by skeletal bond breakage as is found for metal clusters as well as boranes [36–38]. Extrusion of H_2 leads to reformation of the skeletal bond [5,39]. Thus, a reasonable pathway for the reaction of **1** is addition of the alkyne to the basal ruthenium atom on the open face of **1** thereby breaking the Ru–Ru interaction (Scheme 1). Nucleophilic attack of the coordinated alkyne accompanied by loss of H_2 and skeletal rearrangement generates **2**.

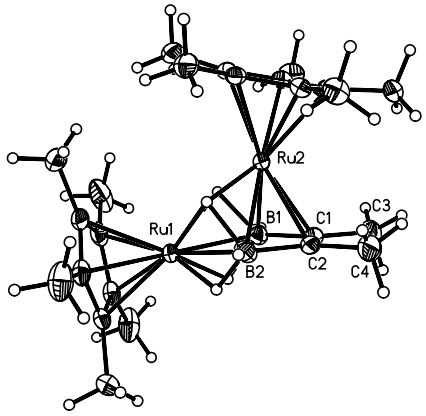

Fig. 2. Molecular structure (50% thermal ellipsoids) of *nido*-1,2-$(Cp^*RuH)_2$-4,5-Me_2-4,5-$C_2B_2H_4$ (**3**). Selected bond lengths (Å) and angles (°): Ru(1)–B(2) 2.375(2), Ru(1)–B(1) 2.378(2), Ru(2)–C(2) 2.2108(19), Ru(2)–C(1) 2.220(2), Ru(1)–Ru(2) 2.9420(5), Ru(2)–B(2) 2.349(2), Ru(2)–B(1) 2.351(2), C(1)–C(2) 1.408(3), C(1)–C(3) 1.523(3), C(2)–C(4) 1.512(3), C(1)–B(1) 1.546(3), C(2)–B(2) 1.556(3), C(2)–B(2)–Ru(1) 112.04(16), C(1)–B(1)–Ru(1) 112.88(16).

2.2. *nido*-1,2-$(Cp^*RuH)_2$-4,5-Me_2-4,5-$C_2B_2H_4$ (**3**)

Taken together, two minor products isolated from the reaction of **1** with 2-butyne turn out to be equally interesting. The first, **3**, is isolated both at room temperature and 85 °C. The spectroscopic data and X-ray structure determination (Fig. 2) show it to be eight sep *nido*-1,2-$(Cp^*Ru)_2(\mu\text{-}H)_2$-4,5-$Me_2$-4,5-$C_2B_2H_5$ and, thus, analogous to the major product of the reaction of **1** with HC≡CC(O)OMe (see above). In terms of stoichiometry, **3** results from the addition of one alkyne and the loss of the elements of BH_3. It is important to note that pyrolysis of **2** does not yield **3** by loss of [BH] as might be assumed (see below also). Hence, the pathway leading to **3** must parallel that leading to **2**.

Before describing its isomeric coproduct, the characteristic multiplicities of the skeletal hydrogens associated with the dimetal fragment in the proton NMR are described as they are characteristic of a structural

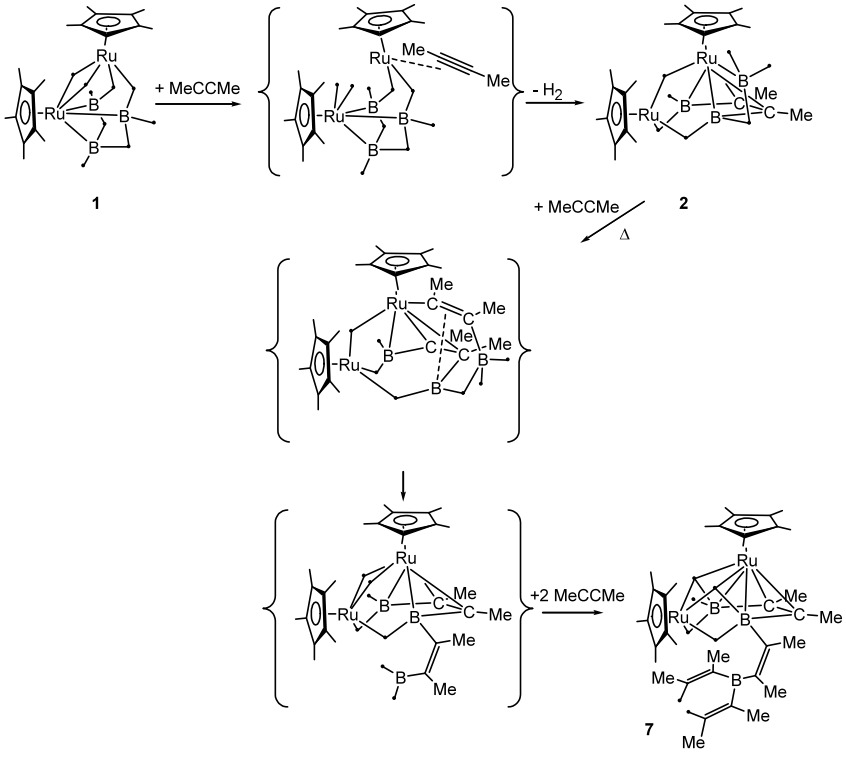

Scheme 1.

feature that appears often in this chemistry. The $^{1}H\{^{11}B\}$-NMR shows a B–Ht resonance (dd, $J_1 = J_2 = 6.4$ Hz), a Ru–H(B)–Ru resonance (dd, $J_1 = J_2 = 6.4$ Hz), and a B–H–Ru resonance (dd, $J_1 = J_2 = 6.4$ Hz). This constitutes the NMR signature of the associated Ru_2B_2 fragment. In addition, the broad signal in the ^{13}C spectrum found for **3** at 109.2 ppm is characteristic of the presence of the skeletal carbon atoms.

2.3. *nido*-1,2-(Cp*RuH)$_2$-4-Et-4,5-$C_2B_2H_5$ (**4**)

The second minor product, **4**, that accompanies **3** under all conditions explored was difficult to isolate. It has the same mass and very similar properties to **3**. Eventually repeated chromatography produced a pure sample that yielded good spectroscopic data and an X-ray structure (Fig. 3). The fact that it is an isomer of **3** was not a surprise. What was a surprise is that it is a product one might expect to generate from 1-butyne rather than 2-butyne.

The solid state structure is fully in accord with the solution spectroscopic data. The ^{1}H spectrum shows a triplet for CH_3 in CH_2CH_3 and two separate multiplets for the two unequal methylene protons in the CH_2CH_3 due to coupling with the adjacent CH_3 and the proton of the C–H fragment. Due to the enhanced relaxation caused by the adjacent boron nucleus, the coupling to the CH_2 is obscured by the broadness of the C–H resonance. The ^{13}C-NMR spectrum corroborates the proton NMR. The CH_2CH_3 carbons are easily assigned and the broad C–H resonance can be distinguished from the quaternary carbon adjacent to a boron atom by its enhanced intensity. The 2D ^{13}C–^{1}H heteronuclear correlation spectrum relates the two separate protons of the methylene group of the CH_2CH_3 with one carbon at 33.2 ppm.

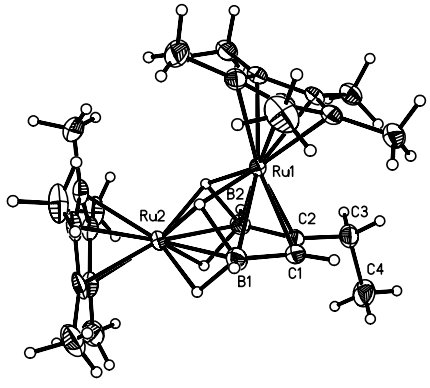

Fig. 3. Molecular structure (50% thermal ellipsoids) of *nido*-1,2-(Cp*RuH)$_2$-4-Et-4,5-$C_2B_2H_5$ (**4**). Selected bond lengths (Å) and angles (°): Ru(1)–B(1) 2.352(5), Ru(1)–B(2) 2.360(4), Ru(1)–Ru(2) 2.9403(5), C(1)–C(2) 1.395(6), C(1)–B(1) 1.537(6), B(1)–Ru(2) 2.400(5), Ru(2)–B(2) 2.386(5), C(2)–C(3) 1.518(5), C(2)–B(2) 1.554(6), C(3)–C(4) 1.537(6), C(2)–B(2)–Ru(2) 111.8(3), C(1)–B(1)–Ru(2) 111.4(3).

The origin of **4** concerned us next. The yields of **4** reach 8–10% even though 1-butyne could not be observed by NMR in the 2-butyne starting material. We are forced to conclude that the alkyne effectively rearranges during its incorporation into the cluster. Although the isomerization of internal alkenes to terminal alkenes by hydroboration/dehydroboration cycles is well known [40], isomerization of alkynes has not been reported. Related complex chemistry occurs when alkenyl-pentaboranes are formed from B_5H_9, i.e. 2-butyne is converted thermally into 2-Me-3-Et-2-CB_5H_7 [41].

A possible pathway to **3**, related to that in Scheme 1, is shown in Scheme 2. Coordination of the alkyne to the apical Ru center and opening of a Ru–B edge leads to the first intermediate shown. Displacement of the unique boron atom of **1** as BH_3 and insertion of the C_2 fragment leads directly to **3**.

The route to **4** is more problematical; however, the suggestion sketched in Scheme 2 is possible. Hydroboration at the unique boron site and coordination to the other (apical) ruthenium center leads to the intermediate shown. Hydroruthenation generates the desired ethyl group and dehydroboration generates the vinyl group shown. In doing so a borane fragment is exposed and displacement of BH_3 in the manner suggested for the reaction of some Lewis bases with B_2H_6 [42] followed by insertion of the C_2 fragment into the cluster leads directly to **4**. What is notable here is the mild conditions which produce **4**. For example, the transformation of alkenyl-pentaboranes into monocarboncarboranes, mentioned above, was carried out above 200 °C [41,43].

2.4. *closo*-1,2-(Cp*RuH)$_2$-4,5-Me_2-4,5-$C_2B_3H_3$ (**5**)

If the fate of **2** on heating is not the production of **3** or **4**, then what is it? Mild thermolysis (85 °C) produces two products. The first, **5**, exhibits a molecular formula consistent with a *closo* seven atom cluster. If static, the NMR data require plane of symmetry with pairs of equivalent boron and carbon atoms plus a unique boron atom and two unique Ru atoms in the cluster skeleton. The two equivalent hydrogens triply bridging Ru_2B faces (chemical shift and coupling pattern) require the structure shown in Scheme 3. The X-ray structure analysis in the solid state (Fig. 4) confirms a *closo*-$Ru_2C_2B_3$ metallacarborane.

For steric reasons, reinsertion of the borane fragment of **2** on thermolysis is most likely at the open face of the *nido* structure. Doing so with retention of all hydrogen atoms would generate a *nido* seven atom metallacarborane which would be expected to exhibit a dodecahedral geometry with one vertex unoccupied. Apparently this compound is not stable under the reaction conditions and H_2 elimination generates the observed *closo* pro-

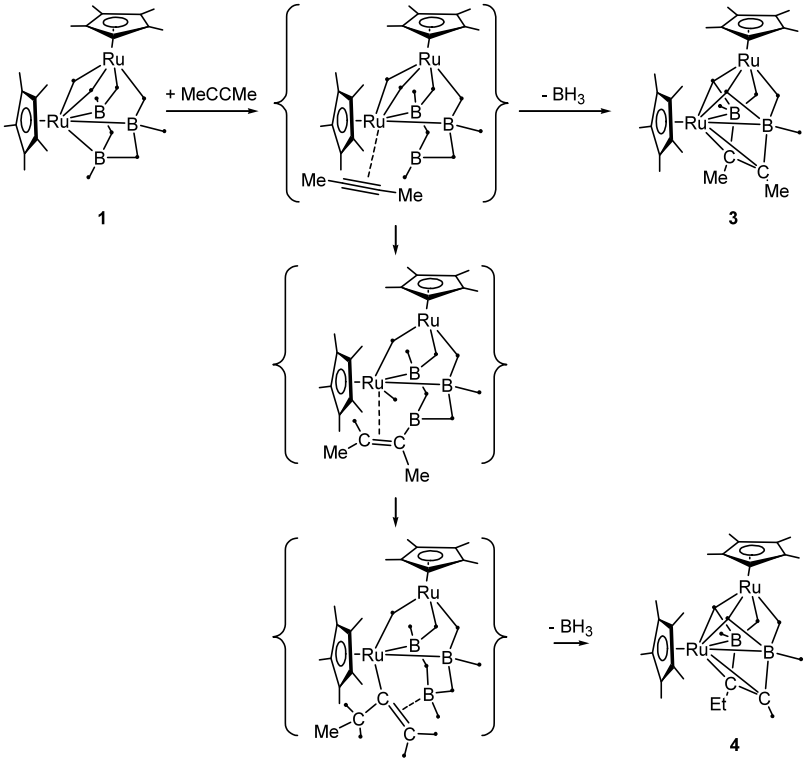

Scheme 2.

duct. This is perfectly consistent with known main group and transition metal cluster chemistry [4].

2.5. *nido*-1,6-(Cp*Ru)$_2$-4,5-Me$_2$-4,5-C$_2$B$_2$H$_6$ (6)

The second product formed on heating **2** is compound **6** (Scheme 3). The molecular formula is identical to that found for **3**; however, the NMR data show that it cannot be **3**. Therefore, it must be an isomer. For a static structure, NMR data show a higher symmetry than found for **5**—pairs of Ru, C, and B atoms are equivalent. Although reasonable structures can be proposed, a solid-state structure was required to unambiguously define the structure as a six atom *nido* framework based on a pentagonal bipyramid with one equatorial atom missing (Fig. 5). Both **3** and **6** are thermally stable and no interconversion was observed on heating at 90 °C for 48 h.

The formation of **6** is noteworthy from several perspectives. First, compounds **3** and **6** are structural isomers of a type not seen before for *nido* clusters with identical compositions. Both are based on a pentagonal bipyramid with five and four connectivity vertices removed, respectively. The former is the expected

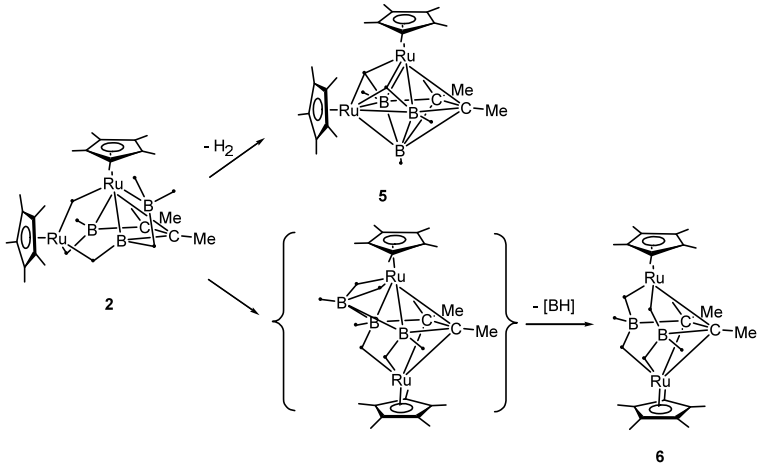

Scheme 3.

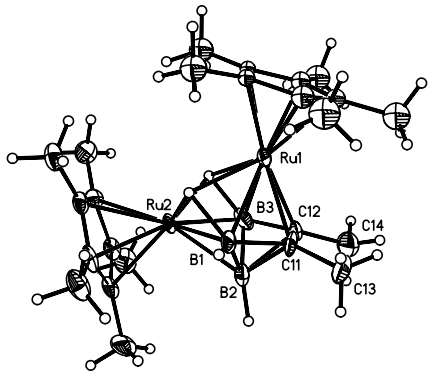

Fig. 4. Molecular structure (50% thermal ellipsoids) of *closo*-1,2-(Cp*RuH)$_2$-4,5-Me$_2$-4,5-$C_2B_3H_3$ (**5**) (major component of the disorder only). Selected bond lengths (Å) and angles (°): Ru(2)–B(1) 2.196(9), R(2)–B(2) 2.172(11), Ru(2)–B(3) 2.180(11), Ru(1)–Ru(2) 2.8832(9), B(1)–C(11) 1.573(13), B(1)–B(2) 1.802(17), B(2)–C(11) 1.738(15), B(2)–C(12) 1.751(12), B(2)–B(3) 1.813(18), B(3)–C(12) 1.582(14), C(11)–C(12) 1.411(15), C(11)–C(13) 1.512(13), C(12)–C(14) 1.541(13), C(11)–B(1)–Ru(2) 112.8(7), C(12)–B(3)–Ru(2) 112.4(7).

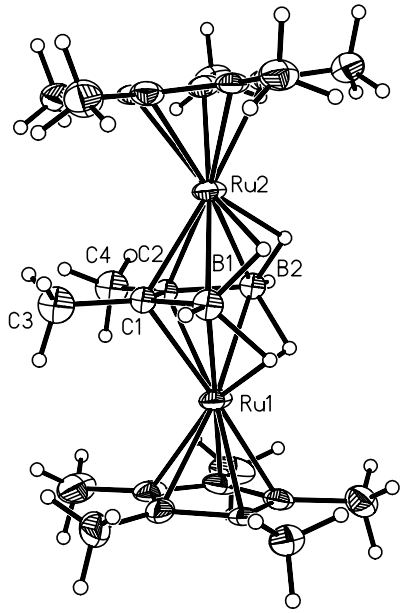

Fig. 5. Molecular structure (50% thermal ellipsoids) of *nido*-1,6-(Cp*Ru)$_2$-4,5-Me$_2$-4,5-$C_2B_2H_6$ (**6**) (major component of the structural disorder only). Selected bond lengths (Å) and angles (°): Ru(1)–C(1) 2.197(7), Ru(1)–C(2) 2.271(8), Ru(1)–B(1) 2.290(8), Ru(1)–B(2) 2.425(8), Ru(2)–C(1) 2.200(7), Ru(2)–C(2) 2.284(8), Ru(2)–B(1) 2.286(8), Ru(2)–B(2) 2.424(8), B(1)–C(1) 1.543(12), B(2)–C(2) 1.593(12), C(1)–C(2) 1.455(11), C(1)–C(3) 1.512(11), C(2)–C(4) 1.503(12), Ru(1)–Ru(2) 3.6383(5), C(2)–C(1)–B(1) 119.3(7), C(1)–C(2)–B(2) 116.7(7).

situation; albeit the number of skeletal hydrogen atoms can affect the preferred geometry [44]. Here the number of bridging hydrogen atoms is identical, yet two stable skeletal forms are observed. Second, the two isomers are produced by two different stoichiometric pathways. Complex **3** is generated by loss of [BH_3] on addition of alkyne whereas **6** is formed by loss of [BH] from **2** which contains an *exo*-polyhedral borane fragment formed on addition of alkyne to **1**. If nothing else, it is clear that the reaction pathway, kinetics and mechanism control, of the two isomers is generated. Third, the specific structural difference between **3** and **6** consists of the interchange of two Ru–H–Ru interactions for two Ru–H–B interactions. We observed earlier in the isoelectronic Rh analog of **1** the presence of two tautomeric forms of the *nido* square-pyramidal differing by the interchange of one Rh–H–Rh for Rh–H–B [45]. In this case, the interconversion was rapid at room temperature and the free energy difference between isomeric forms was only $\approx$400 cal mol^{-1}. Of course there is only a single way of generating a *nido* framework from the base octahedron so both tautomers have the same skeletal shape.

Insertion of the *exo*-framework borane fragment into the open face of **2** was suggested to lead to **5**. The Ru–Ru edge also constitutes a potential site for insertion of the *exo*-borane fragment of **2**. Insertion here would formally generate a *nido* seven atom cluster which should be based on a dodecahedron with one missing vertex. One possibility is shown in Scheme 3 where it is a vertex of connectivity four that is left vacant. Loss of [BH] leads easily to **6**. [BH] fragment loss is frequently observed in borane and metallaborane chemistry, however, little information on the fate of the [BH], can be found in the literature [46–48].

2.6. *nido*-1,2-(Cp*RuH)$_2$-3-{CMeCMeB(CMeCHMe)$_2$}-4,5-Me$_2$-4,5-$C_2B_2H_3$ (7)

If **1** is heated at 85 °C in the presence of an excess of alkyne, **7** is isolated as the major product along with **3**, **4**, **5** and **6** as minor products. Note that *pileo*-2,3-(Cp*Ru)$_2$(μ-H)B_4H_7 is generated from the side product *nido*-1,2-(Cp*RuH)$_2B_4H_8$ in all reactions involving the heating of **1** above 60 °C [4]. Thermolysis of **2** in the presence of excess of 2-butyne (Scheme 1) generates **7** showing that **2** is an intermediate in its formation. The molecular mass of **7** corresponds to a molecular formula $C_{36}H_{61}B_3Ru_2$ which shows that the addition of three more alkynes has occurred. Unfortunately all attempts to grow crystals of **7** for a structure determination were not successful as in solution it slowly is transformed into an insoluble powder. As **7** is the ultimate product of the reaction of **1** with 2-butyne, sufficient multinuclear, 1 and 2D-NMR data were obtained to define the structure.

The NMR data of **7** immediately suggest a similarity to **3**, albeit with symmetry broken by the presence of an *exo*-cluster organic substituent. Thus, the ^{1}H-NMR spectrum (Fig. 6) shows two types of Cp*, two Ru–H(B)–Ru and two B–H–Ru. The $^1H\{^{11}B\}$- and ^1H–^1H-COSY experiments confirm the presence of characteristic (see above) triply-bridged protons via observed coupling of the metal hydrides with the B–

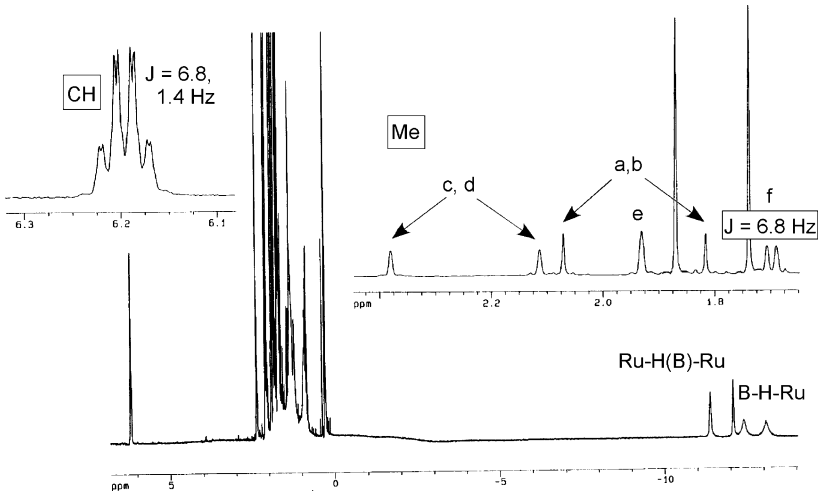

Fig. 6. ^{1}H-NMR spectrum of *nido*-1,2-(Cp*RuH)$_2$-3-{CMeCMeB(CMeCHMe)$_2$}-4,5-Me$_2$-4,5-$C_2B_2H_3$ (**7**) at 25 °C in C_6D_6.

H–Ru protons. A *nido* six atom cluster framework containing two boron atoms is suggested. However, the ^{11}B spectrum shows three different boron atoms in the ratio of 1:1:1, two of which are clearly cluster based. The boron resonance at 66.2 ppm is very broad and nearly 70 ppm down-field of other two. It is most reasonably assigned to a tricoordinate boron center with low symmetry, which must constitute part of the *exo*-cluster fragment. The ^{13}C spectrum (Fig. 7) reveals the two framework carbon atoms attached to B (broad, at 101.5 and 109.8 ppm). Generation of skeletal framework **7** from **2** suggests that the *exo*-cluster substituent was generated from the *exo*-BH_2 group of **2**.

Taking this tack, the remaining signals of **7** were successfully assigned to a chemically reasonable organoborane fragment (Fig. 8). One quartet of quartets ($J_1 = 1.4$ Hz, $J_2 = 6.8$ Hz) of intensity 2 in the olefinic region is assigned to two (=C–H) fragments. Including the cluster framework methyl groups, six types of methyl groups are observed with a total intensity of 24. This is confirmed by the ^{13}C-NMR data in Fig. 7.

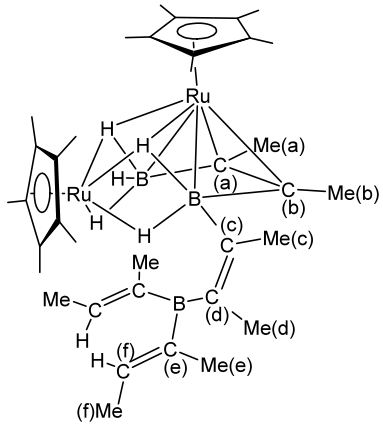

Fig. 8. Postulated structure of *nido*-1,2-(Cp*RuH)$_2$-3-{CMeCMeB(CMeCHMe)$_2$}-4,5-Me$_2$-4,5-$C_2B_2H_3$ (**7**).

The methyl resonances can then be grouped into four sets. One type of two sharp methyl resonances is easily assigned to the methyl groups on the cluster framework by comparison with **3**. Of the other three distinctly

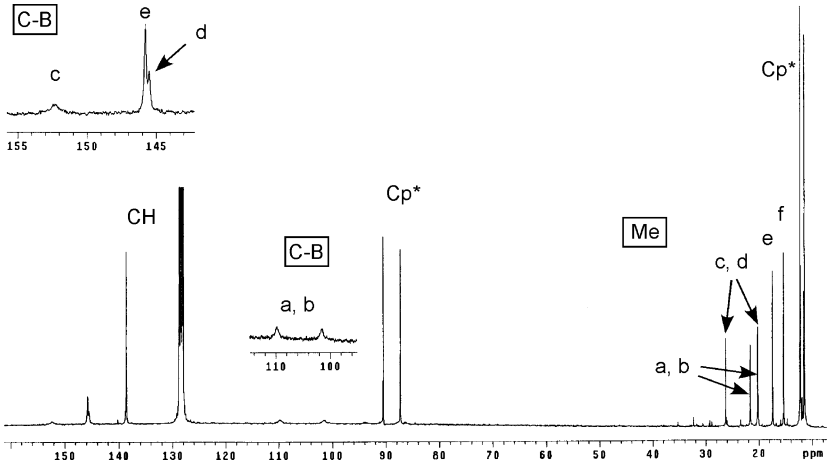

Fig. 7. ^{13}C-NMR spectrum of *nido*-1,2-(Cp*RuH)$_2$-3-{CMeCMeB(CMeCHMe)$_2$}-4,5-Me$_2$-4,5-$C_2B_2H_3$ (**7**) at 25 °C in C_6D_6.

broader sets of resonances, the first corresponds to two equivalent methyl groups, the second corresponds to two inequivalent methyl groups, and the third corresponds to two equivalent methyl groups with the resonance split by a coupling of 6.8 Hz. The $^{1}H-^{1}H$-COSY establishes a correlation between one quartet of the =CH group and the doublet of the CH_3 group ($J_2 = 6.8$ Hz). The smaller coupling observed for the =CH resonance ($J_1 = 1.4$ Hz) can be assigned to a CH_3 four bonds away. The methyl resonance is too broad to reveal this small coupling. A $^{13}C-^{1}H$ heteronuclear correlation experiment relates the doublet in the methyl region to the carbon signal of the two identical methyl groups. In addition this experiment connects the intensity 2 quartet of quartets to a sharp olefinic carbon signal at 140 ppm. Two signals of unequal intensity in the ^{13}C-NMR at 145.5 (1C) and 145.8 (2C) ppm, are assigned to three olefinic carbon atoms around the tricoordinate, *exo*-framework boron atom. The broad signal at very low field (152.5 ppm) is assigned to an olefinic carbon atom linked to the framework boron atom. The complete assignment of the spectra shown in Figs. 6 and 7 is given in the correspondingly labeled structure shown in Fig. 8.

Consistent with the involvement of the *exo*-BH_2 group of **2**, **7** forms from **2** but not **3**, **4**, **5** or **6**. A reasonable, but not exclusive, pathway for its formation is shown in Scheme 1. Insertion of the alkyne into the Ru–B edge bond, reminiscent of the insertion of an alkyne into a Pt–B bond [49,50], leads to the first intermediate shown. Bond metathesis and skeletal hydrogen rearrangement leads to an *exo*-cluster vinyl borane. Presumably this is a stable species; however, in the presence of excess alkyne it would undergo rapid hydroboration to yield the observed product **7**.

2.7. *closo*-1,7-(Cp*Ru)$_2$-2,3,4,5-Me$_4$-6-(CHMeCH$_2$Me)-2,3,4,5-C$_4$B (**8**)

There are some minor products formed along with **3**, **4**, **5**, **6**, **7** in the high temperature reaction mixture. A particularly interesting one is **8** for which the spectroscopic data suggested an unusual cluster structure. Fortunately an X-ray structure was obtained (Fig. 9) and shows **8** to be a normal eight sep, *closo* seven atom metallacarborane. It is also a 30 valence electron triple-decker complex in which the middle ring is a planar borone ligand—that is, a five-membered ring containing one boron and four carbon atoms [51]. Many *closo*-frameworks and triple-decker complexes are very stable and, hence, likely thermodynamic products. The spectroscopic data are all consistent with the X-ray structure including the saturated organic substituent attached to the single boron atom.

The NMR justification for the 2-butyl substituent on **8** is worth mentioning. The ^{1}H-NMR spectrum shows

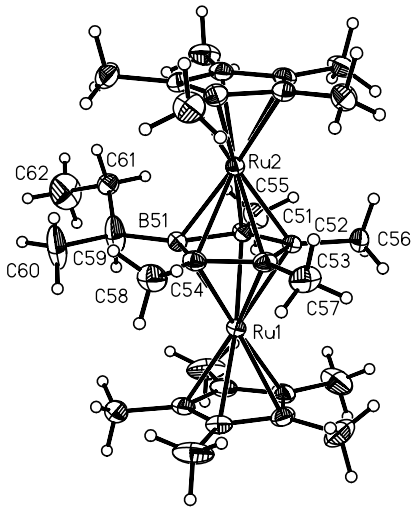

Fig. 9. Molecular structure (50% thermal ellipsoids) of *closo*-1,7-(Cp*Ru)$_2$-2,3,4,5-Me$_4$-6-(CHMeCH$_2$Me)-2,3,4,5-C$_4$B (**8**) (major component of the structural disorder only). Selected bond lengths (Å) and angles (°): Ru(1)–C(53) 2.186(2), Ru(1)–C(52) 2.199(2), Ru(1)–C(54) 2.218(2), Ru(1)–C(51) 2.220(2), Ru(1)–B(51) 2.280(3), Ru(2)–C(53) 2.185(2), Ru(2)–C(52) 2.191(2), Ru(2)–C(54) 2.212(2), Ru(2)–C(51) 2.223(2), Ru(2)–B(51) 2.288(3), B(51)–C(51) 1.585(3), B(51)–C(54) 1.588(3), B(51)–C(59) 1.593(4), C(51)–C(52) 1.469(3), C(52)–C(53) 1.481(3), C(53)–C(54) 1.482(3), C(54)–C(58) 1.505(3), C(59)–C(61) 1.454(5), C(59)–C(60) 1.542(4), C(61)–C(62) 1.517(14), C(51)–B(51)–C(54) 101.43(19), C(52)–C(51)–B(51) 110.45(19), C(51)–C(52)–C(53) 109.09(19), C(52)–C(53)–C(54) 109.48(19), C(53)–C(54)–B(51) 109.54(19).

four types of methyl groups containing two singlets, one doublet and one triplet. The CH, CH_2 hydrogen atoms are unambiguously assigned on the basis of $^{1}H-^{1}H$-COSY which shows the coupling to the two methyl groups as well as the presence of weak coupling between the CH proton and one methylene proton of the $MeCH_2$ fragment. Details of the formation of **8** are not known but the overall path is not a mystery. Addition of alkyne to **3** with extrusion of [BH_3] concomitant with incorporation of another alkyne at the lone boron atom and reduction by the remaining three hydrogen atoms generate **8**. Hydroboration and hydrogen transfer from metallaboranes or metallacarboranes to alkynes are readily observed in the case of terminal alkynes, i.e. HC≡CPh (see below) and HC≡CC(O)OMe [52,53].

Considering the rich reaction chemistry of the simple internal alkyne already described, we were interested in variations that might be generated by a terminal alkyne. Phenylacetylene was chosen—it is a typical terminal alkyne often used in cluster chemistry. Three new compounds were isolated. One is distinctly different from those formed from the representative internal alkyne whereas the other two are similar albeit with interesting variations.

2.8. *nido*-1,2-(Cp*Ru)$_2$(μ-H)(μ-CHCH$_2$Ph)B$_3$H$_6$ (**9**)

Reaction of **1** with phenylacetylene at ambient temperature leads to the isolation of **9**. The spectroscopic data show that a single alkyne had been added without loss of H_2 or BH_3. Consistent with no mass loss, these data also suggest that the cluster framework of **1** remains intact, i.e. insertion of the alkyne has not occurred. In addition to one Ph group, the ^{1}H-NMR spectrum of **9** contains three resonances corresponding to saturated aliphatic C–H protons. These C–H resonances exhibit informative ^{1}H–^{1}H splitting. In order of increasing field strength, there is a doublet of doublets ($J_1 = 3.9$ Hz, $J_2 = 12.1$ Hz), a broad doublet ($J = 12.1$ Hz), which indicates proximity to a quadrupolar boron atom, and a doublet of doublets ($J_1 = J_2 = 12.1$ Hz). Assignment to a B–CH–CH$_2$Ph fragment with a diastereotopic methylene moiety is straightforward. However, without a structural precedent the spectroscopic data were not sufficient to unambiguously define the actual structure of **9**.

Fortunately, suitable crystals for a solid-state structure determination were obtained and the structure solution (Fig. 10) reveals that the added alkyne has been converted to a μ-alkylidene fragment. Comparing the number and type of framework hydrogen atoms in **1** and **9** suggests that the two additional hydrogen atoms required to generate the alkylidene fragment most likely arise from one terminal B–H and one bridging Ru–H–Ru of **1**. Hence, **9** may be considered as arising from hydroboration and hydroruthenation. Both reactions are known but reaction of terminal alkynes with **1** provides the first instance of joint operation on a single substrate molecule [28]. Note that the formation of **9** with the framework of **1** requires no change in the number of sep. Since a two-electron μ-alkylidene ligand replaces two one-electron hydrogen atoms, **9** still retains a seven sep *nido* diruthenapentaborane structure. Unlike HC≡CC(O)OMe [28], the regiochemistry of HC≡CPh reduction is anti-Markovnikoff and the Markovnikoff products are not isolated. Although M–M bridging CR$_1$R$_2$ fragments constitute important ligand types in transition metal organometallic chemistry [15], this work suggests that M–B bridging CR$_1$R$_2$ fragments are also possible.

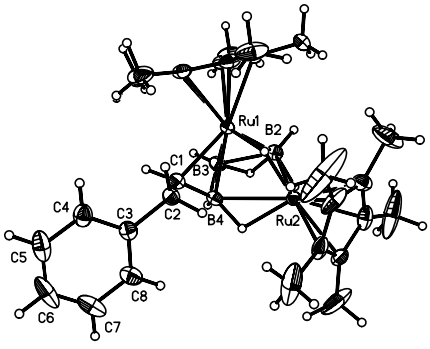

Fig. 10. Molecular structure (50% thermal ellipsoids) of *nido*-1,2-(Cp*Ru)$_2$(μ-H)(μ-CHCH$_2$Ph)B$_3$H$_6$ (**9**). Selected bond lengths (Å) and angles (°): Ru(1)–B(3) 2.126(3), Ru(1)–B(4) 2.144(3), Ru(1)–B(2) 2.170(3), Ru(1)–C(1) 2.230(2), Ru(1)–Ru(2) 2.8643(3), C(1)–B(4) 1.499(4), C(1)–C(2) 1.522(4), Ru(2)–B(2) 2.310(3), Ru(2)–B(4) 2.402(3), C(2)–C(3) 1.518(4), B(4)–C(1)–C(2) 122.6(2), B(4)–C(1)–Ru(1) 66.90(14), C(2)–C(1)–Ru(1) 120.41(17), C(3)–C(2)–C(1) 109.3(2).

The pathway for the formation of **9** from **1** is of interest but we were unable to obtain any direct information. One relevant point is that another compound is formed along with **9**. It has a similar polarity to **9** but, due to its instability, we were only able to obtain good ^{1}H- and ^{11}B-NMR data. However, the information obtained is sufficient to provide a reasonable structure for **10**. One can simply count the number of protons and boron atoms: two Cp*, two B–H, two B–H–B, two B–H–Ru, two Ru–H–Ru, one Ph, one CH$_2$ and three B. Given the data on **9**, it appears that **10** is formed by a single reduction by one B–H. The difference with **9** is that **10** possesses one additional Ru–H–Ru and the H added to the alkyne generates a CH$_2$ group. The chemical shift of the latter is a couple of ppm upfield from where one expects and uncoordinated olefin. Thus, as shown in Scheme 4, weak coordination to the adjacent metal center is suggested.

Most likely this Markovnikoff product of a single hydrometallation is not an intermediate in the formation of **9**. Complex **10** differs from the analogous putative precursor to **9** by placement of the phenyl group one carbon atom closer to the cage. Hence, a steric factor may well prevent the orientation necessary for the second hydrometallation. Unfortunately, without a solid state structure of **10**, it is not possible to define this factor.

2.9. *nido*-1,2-(Cp*Ru)$_2$(μ-H)(μ-BH$_2$)-3-(CH$_2$)$_2$Ph-4-Ph-4,5-C$_2$B$_2$H$_4$ (**11**)

Another product isolated from the room temperature reaction results from the addition of two phenyl acetylenes (Scheme 4). The composition and structure of **11** are established from the spectroscopic data by comparison with compounds with similar structural components and for which solid state X-ray diffraction studies are available. The exact mass measurement of **11** gives a molecular ion corresponding to C$_{36}$H$_{51}$B$_3$Ru$_2$. The ^{11}B spectrum shows three types of boron atoms in a 1:1:1 ratio. The ^{1}H-NMR spectra reveal that **11** has two Ph groups, two types of Cp*, two types of B–H, one B–C–H (singlet), two types of CH$_2$ (multiplets), one B–H–B, two types of B–H–Ru, and one Ru–H–Ru.

The postulated structure is shown in Fig. 11 and contains an inserted alkyne accompanied by an *exo*-

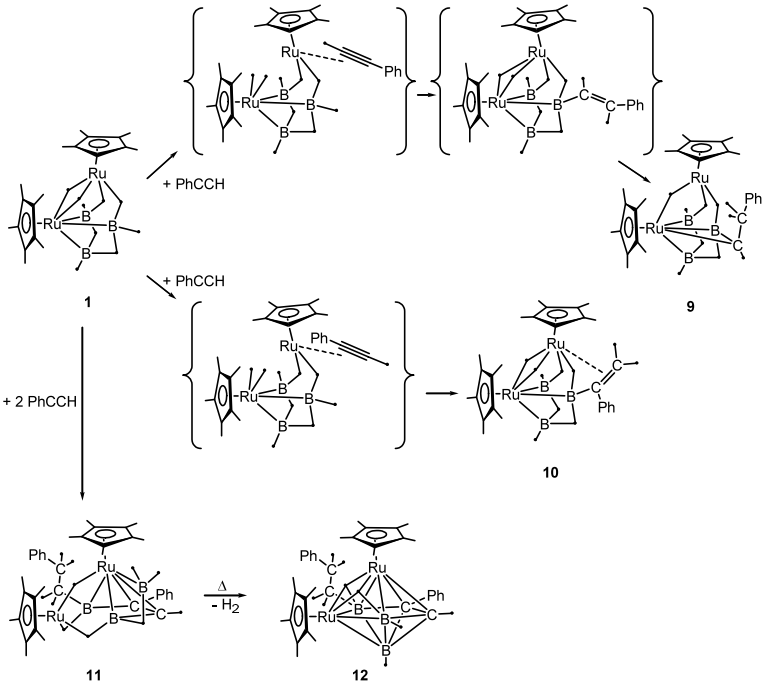

Scheme 4.

framework BH_2 for which **2** is a model. There are two orientations possible for insertion of the alkyne into the cluster and the one shown has been established by a $^1H\{^{11}B\}-^1H\{^{11}B\}$-COSY experiment. The 2D spectrum shows correlations of the unique B–H–B with one of the BH_2 protons and the C–H proton. This shows that the C–H must be adjacent to the boron atom to which the *exo*-BH_2 is attached. The boron *exo*-cluster substituent formed by full reduction of the second phenyl acetylene is clear from the absence of one B–H proton signal and the presence of signals characteristic of a CH_2CH_2Ph fragment.

2.10. *closo*-1,2-(Cp*RuH)$_2$-3-(CH$_2$)$_2$Ph-4-Ph-4,5-C$_2$B$_3$H$_3$ (**12**)

Additional evidence for the structure of **11** results from its thermolysis at 90 °C. The thermolysis of **11** is monitored by NMR to show that it is the precursor to **12**. The ^{11}B-NMR spectrum of **12** shows three boron resonances. The ^1H-NMR spectra reveal that **12** has two Ph groups, two types of Cp*, two types of B–Ht, one B–C–H, two groups of CH_2(multiplets), two types of B–H–Ru or Ru–H(B)–Ru. The $^1H\{^{11}B\}-^1H\{^{11}B\}$-COSY exhibits correlation of the two Cp* with the two high-field signals, which tells us there are two Ru–H(B)–Ru rather than two B–H–Ru protons. There is also a correlation between one of the Ru–H(B)–Ru protons and the C–H but not between the C–H proton and the adjacent B–H proton as observed for **11**. This negative result does not imply a different connectivity since coupling strength is dependent on the dihedral angle of the two bonds among other things. Although the C–H and C–Ph fragments could exchange during pyrolysis, we have no evidence that they do. The proposed structure is shown in Fig. 11.

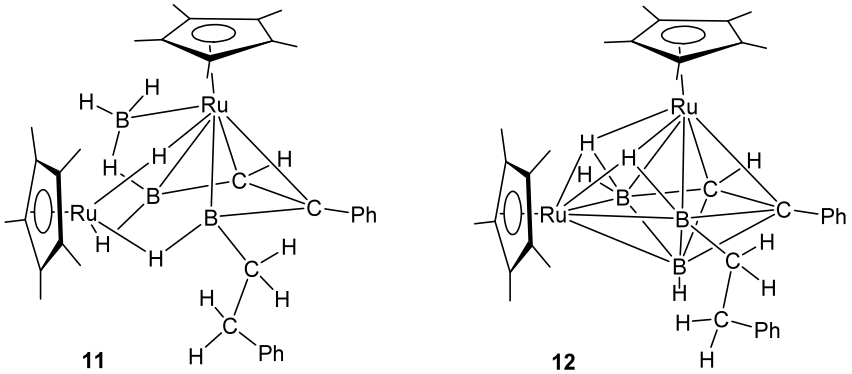

Fig. 11. Postulated structures of *nido*-1,2-(Cp*Ru)$_2$(μ-H)(μ-BH$_2$)-3-(CH$_2$)$_2$Ph-4-Ph-4,5-C$_2$B$_2$H$_4$ (**11**) and *closo*-1,2-(Cp*RuH)$_2$-3-(CH$_2$)$_2$Ph-4-Ph-4,5-C$_2$B$_3$H$_3$ (**12**).

The formation of **11** and its subsequent conversion into **12** on heating connects the reaction of **1** with phenyl acetylene to the reaction with 2-butyne. The products are not identical but **11** is an analog of **2**, with one B–R rather than B–H group in the base and the conversion into **12** is analogous to the conversion of **2** into **5**.

Alkyne insertion, formation of *exo*-BH_2, and loss of 2H occur for both internal and terminal alkynes; however, in the former case H_2 is lost whereas in the latter the 2H are taken up by another alkyne on hydroboration of a B–H. In addition, reaction of **1** with the terminal alkyne competitively forms a bridging alkylidene. The postulated intermediate in the formation of the bridging alkylidene ligand (Scheme 4) may well also be an intermediate in the formation of the saturated group on the B–R fragment of **11**.

3. Conclusions

An alternative route to ruthenacarboranes has been developed based on the reaction of *nido*-1,2-$(Cp^*Ru)_2B_3H_9$ with internal and terminal alkynes. The reactions proceed smoothly at ambient temperature to yield products understandably related to the starting materials. At higher temperatures more complex chemistry is observed with the formation of more stable products. The metallaborane to metallacarborane route is more than an alternative to the carborane to metallacarborane route as the products of the former reveal novel structural chemistry in species that are intermediates in the generation of more stable frameworks. Hence, they are mechanistically suggestive in a broad sense. The two ''extra'' framework hydrogens of **1** required to make up for the two one electron Cp*Ru fragments appear to be crucial in generating the low barrier for reaction with alkynes. Some chromaboranes, rhenaboranes, rhodaboranes, iridaboranes, and even other ruthenaboranes that do not possess this structural feature do not react with alkynes under such mild conditions.

4. Experimental

4.1. Synthesis

All operations were conducted under argon atmosphere using standard Schlenk techniques [54]. Solvents were dried with appropriate reagents and distilled before use under N_2. $LiBH_4$ (2 M in THF), MeC≡CMe, PhC≡CH (Aldrich), and $[(Cp^*RuCl_2)_n]$ (Strem) were used as received. *nido*-1,2-$(Cp^*Ru)_2B_3H_9$ (**1**) was prepared according to the literature procedures [4]. Silica gel (ICN 32–63, 60 Å) was purchased from ICN Biomedicals GmbH and predried at 180 °C before use. NMR spectra were recorded on a Bruker AMX 400 or a Varian 500 FT-NMR spectrometers. The solvent resonances were used as reference: ^1H (δ, ppm, benzene-d_6, 7.16); and ^{13}C (δ, ppm, benzene-d_6, 128.39). For ^{11}B an external reference was used: a sealed capillary containing $[(Me_4N)(B_3H_8)]$ in acetone-d_6 (δ_B, ppm, −29.7). Infrared spectra were measured on a Perkin–Elmer Paragon 1000 FTIR spectrometer. Mass spectra were obtained on a JEOL LMS-AX505 mass spectrometer using the EI or FAB ionization modes. MALDI spectra were obtained on a Voyager-DE Biospectrometry workstation.

4.2. Procedures and spectroscopic data

2, **3**, **4**: To the orange solution of **1** (150 mg, 0.29 mmol) in hexane (40 ml) was added MeC≡CMe (0.8 g, 14.8 mmol). The resulting mixture was stirred for 24 h at ambient temperature during which the color of the solution changed into orange–red. After removal of solvent and excess alkyne, the residue was chromatographed. Elution with hexane:toluene (20:1) gave **2** (83.8 mg, 51%), **3** (27.4 mg, 17%), **4** (13 mg, 8%).

2. NMR ^1H (C_6D_6): 4.44 (br 1H, B–Ht), 3.70 (br 1H, B–Ht), 3.63 (br. 1H, B–Ht), 1.93 (s, 3H, Me), 1.82 (s, 15H, Cp*), 1.80 (s, 3H, Me), 1.61 (s, 15H, Cp*), −3.25 (d, br $J_{B-H} = 65$ Hz, 1H, B–H–B), −11.02 (pcq, 1H, B–H–Ru), −14.92 (s, 1H, Ru–H–Ru), −14.94 (br. 1H, B–H–Ru). ^{11}B (C_6D_6): 26.1, 20.1, 11.4 (1:1:1). ^{13}C (C_6D_6): 10.76 (Cp*), 12.17 (Cp*), 15.01 (Me), 19.98 (Me), 88.71 (Cp*), 93.73 (Cp*), 111.50 (br C–B), 128.30 (br. C–B). FABMS: 564 [M^+ −4H] (100%). IR (KBr, cm^{-1}): 2411, 2461 (ν_{B-H}).

3. NMR ^1H (C_6D_6): 2.12 (s, 6H, Me), 2.05 (br 1H, B–Ht), 1.87 (s, 15H, Cp*), 1.78 (s, 15H, Cp*), −11.52 (br s, 2H, Ru–H–Ru), −12.572 (br 2H, B–H–Ru). ^{11}B (C_6D_6): −16.2. ^{13}C (C_6D_6): 11.49 (Cp*), 12.42 (Cp*), 21.20 (Me), 86.71 (Cp*), 90.37 (Cp*), 108.52 (br C–B). MALDIMS: 556 [M^+]. IR (KBr, cm^{-1}): 2427 (ν_{B-H}).

4. NMR ^1H (C_6D_6): 4.40 (br s, 1H, CH), 2.31 (m, 2H, CH_2), 2.09 (br, 1H, B–Ht), 1.99 (br, 1H, B–Ht), 1.85 (s, 15H, Cp*), 1.79 (s, 15H, Cp*), 1.45 (t, $J = 7.4$ Hz, 3H, CH_3), −11.67 (s, 1H, Ru–H–Ru), −11.83 (s, 1H, Ru–H–Ru), −12.18 (br s, 1H, B–H–Ru), −12.60 (br s, 1H, B–H–Ru). ^{11}B (C_6D_6): −18.2, −14.7 (1:1). ^{13}C (C_6D_6): 11.73 (Cp*), 12.38 (Cp*), 20.79 (Me), 33.18 (CH_2), 86.63 (Cp*), 91.14 (Cp*), 97.54 (br B–C–H) and 118.77 (br C–B). MALDIMS: 556 [M^+]. IR (KBr, cm^{-1}): 2436 (ν_{B-H}).

5, **6**: Complex **2** (96 g, 0.17 mmol) was dissolved in toluene (20 ml) and heated for 24 h at 85 °C under argon. After removal of the solvent, the residue was chromatographed and elution with hexane gave **5** (44.2 mg, 46%) and hexane/toluene (20:1) gave **6** (19.8 mg, 21%).

5. NMR ^{1}H (C_6D_6): 3.82 (pcp, 3H, B–Ht), 2.13 (s, 6H, Me), 2.07 (s, 15H, Cp*), 1.68 (s, 15H, Cp*), −11.12 (s, br 2H, B–H–Ru). ^{11}B (C_6D_6): 11.07, 8.72 (2: 1). ^{13}C (C_6D_6): 11.52 (Cp*), 12.29 (Cp*), 21.25 (Me), 86.24 (Cp*), 87.80 (br, C–B), 93.95 (Cp*). FAB: 563.3 [$M^+ - 3H$] (100%). IR (KBr, cm^{-1}): 2477(ν_{B-H}).

6. NMR ^{1}H (C_6D_6): 2.41 (s, 6H, Me), 1.66 (s, 30H, Cp*), 1.18 (br, 2H, B–H–B), −10.067 (br s, 4H, B–H–Ru). ^{11}B (C_6D_6): −32.9. ^{13}C (C_6D_6): 10.92 (Cp*), 21.00 (Me), 84.63 (Cp*). FAB: 554 [$M^+ - 2H$] (100%). IR (KBr, cm^{-1}): 2420 (ν_{B-H}).

7: Complex **2** (125 mg, 0.22 mmol) and MeC≡CMe (0.8 g, 14.8 mmol) were dissolved in toluene (20 ml) and heated for 24 h at 85 °C under Argon. After removal of solvent the residue was chromatographed. Elution with hexane gave **5** (16.4 mg, 17%) and **7** (92 mg, 58%) and elution with hexane–toluene (20:1) gave **6** (10.5 mg, 11%).

7. NMR ^{1}H (C_6D_6): 6.18 (qq, $J_1 = 1.4$ Hz, $J_2 = 6.8$ Hz, 2H, CH), 2.37 (s, br 3H, Me), 2.10 (s, br 3H, Me), 2.06 (s, 3H, Me), 1.92 (s, br 6H, Me), 1.87 (s, 15H, Cp*), 1.80 (s, 3H, Me), 1.74 (s, 15H, Cp*), 1.69 (d, br $J = 6.8$ Hz, 6H, Me), −11.40 (s, br 1H, Ru–H(B)–Ru), −12.09 (s, br. 1H, Ru–H(B)–Ru), −12.42 (br 1H, B–H–Ru), −13.09 (br 1H, B–H–Ru). ^{11}B (C_6D_6): −2.0, −15.8, 66.2 (1:1:1). ^{13}C (C_6D_6): 11.45 (Cp*), 12.22 (Cp*), 15.37 (2Me), 17.46 (2Me), 20.19 (Me), 20.25 (Me), 21.64 (Me), 26.22 (Me), 87.28 (Cp*), 90.49 (Cp*), 101.48 (br C–B), 109.80 (br. C–B), 138.63 (CH), 145.53 (C), 145.81 (C), 152.45 (br C–B). FAB: 728 [$M^+ - 2H$] (100%). IR (KBr, cm^{-1}): 2417(ν_{B-H}).

8: To **1** (150 mg, 0.29 mmol) in toluene (20 ml) was added MeC≡CMe (0.8 g, 14.8 mmol). The resulting mixture was stirred for 24 h at 85 °C. After removal of solvent and excess alkyne, the residue was chromatographed. Elution with hexane gave **8** (12 mg, 6%), **5** (19 mg, 12%) and **7** (71 mg, 34%) and elution with hexane–toluene (20:1) gave **6** (13 mg, 8%), **3** (22.5 mg, 14%), **4** (14.6 mg, 9%).

8. NMR ^{1}H (C_6D_6): 2.29 (m, 1H, CH_2), 2.13 (s, 6H, Me), 1.83 (s, 6H, Me), 1.76 (m, 1H, CH), 1.63 (m, 1H, CH_2), 1.58 (d, $J = 5.8$ Hz, 3H, Me), 1.55 (s, 30H, Cp*), 1.42 (t, $J = 7.3$ Hz, 3H, Me). ^{11}B (C_6D_6): 7.8. FABMS: [$M^+ + H$] (100%); 651.2226 (measured), 651.2249 (calculated) for $C_{32}H_{52}BRu_2$.

9, **10**, **11**: To **1** (135 mg, 0.26 mmol) in hexane (20 ml) was added PhC ≡ CH (0.35 ml, 3.2 mmol). The resulting mixture was stirred for 14 h at room temperature (r.t.) and after removal of solvent and excess of alkyne the residue was chromatographed. Elution with hexane–

Table 1
Crystallographic data and structure refinement details for compounds **2**, **3**, **4** and **5**

	2	**3**	**4**	**5**
Empirical formula	$C_{24}H_{43}B_3Ru_2$	$C_{24}H_{42}B_2Ru_2$	$C_{24}H_{42}B_2Ru_2$	$C_{24}H_{41}B_3Ru_2$
Formula weight	566.15	554.34	554.34	564.12
Crystal system	Monoclinic	Monoclinic	Monoclinic	Monoclinic
Space group	$P2_1/c$	$P2_1/n$	$P2_1/n$	$P2_1/c$
a (Å)	13.5206(5)	8.3417(4)	15.3419(17)	16.4035(9)
b (Å)	8.8389(3)	20.0354(9)	21.921(2)	16.9484(10)
c (Å)	21.4670(8)	14.9418(7)	16.5445(18)	19.4009(11)
α (°)	90	90	90	90
β (°)	98.9910(10)	95.5040(10)	115.692(2)	110.1600(10)
γ (°)	90	90	90	90
V (Å^3)	2533.94(16)	2485.7(2)	5014.0(10)	5063.3(5)
Z	4	4	4	4
D_{calc} (g cm^{-3})	1.484	1.481	1.469	1.480
$F(000)$	1160	1136	2272	2304
μ (mm^{-1})	1.200	1.222	1.212	1.201
Crystal size (mm)	0.3 × 0.3 × 0.2	0.25 × 0.2 × 0.2	0.25 × 0.25 × 0.15	0.3 × 0.2 × 0.1
θ Range (°)	1.92–25.00	2.03–28.31	1.86–25.00	1.85–25.00
Reflections collected	20 818	26 895	41 098	41 328
Reflections unique [R_{int}]	4452 [0.0182]	6169 [0.0196]	8820 [0.0302]	8915 [0.0320]
Completeness to θ	$\theta = 25.00$, 100%	$\theta = 28.31$, 99.8%	$\theta = 25.00$, 99.9%	$\theta = 25.00$, 100.0%
Max. and min. transmission	1.0000, 0.9033	1.0000, 0.8627	1.0000, 0.7944	1.0000, 0.8875
Refinement method	Full-matrix on F^2	Full-matrix on F^2	Full-matrix on F^2	Full-matrix on F^2
Data/restraints/parameters	4452/0/263	6169/0/253	8820/0/505	8915/0/384
Goodness-of-fit on F^2	1.091	1.059	1.039	1.068
Final R indices [$I > 2\sigma(I)$]	$R_1 = 0.0397$, $wR_2 = 0.0891$	$R_1 = 0.0231$, $wR_2 = 0.0583$	$R_1 = 0.0367$, $wR_2 = 0.0893$	$R_1 = 0.0891$, $wR_2 = 0.2074$
R indices (all data)	$R_1 = 0.0403$, $wR_2 = 0.0894$	$R_1 = 0.0246$, $wR_2 = 0.0592$	$R_1 = 0.0454$, $wR_2 = 0.0936$	$R_1 = 0.1015$, $wR_2 = 0.2161$
Largest difference peak and hole (e Å^{-3})	3.288, −1.814	0.833, −0.421	2.951, −1.141	2.697, −4.173

toluene (20:1) gave **9** (27 mg, 17%) and **10** (24 mg, 15%) and elution with hexane–toluene (10:1) gave **11** (65 mg, 35%).

9. NMR ^{1}H (C_6D_6): 7.41 (m, 2H, Ph), 7.28 (m, 3H, Ph), 3.79 (br 1H, B–Ht), 3.47 (br 1H, B–Ht), 2.96 (dd, $J_1 = 3.9$ Hz, $J_2 = 12.1$ Hz, 1H, CH), 2.73 (d, br $J = 12.1$ Hz, 1H, CH), 2.53 (dd, $J_1 = J_2 = 12.1$ Hz, 1H, CH), 1.80 (s, 15H, Cp*), 1.793 (s, 15H, Cp*), −2.34 (s, br 1H, B–H–B), −3.48 (s, br 1H, B–H–B), −10.53 (s, br 1H, B–H–Ru), −11.32 (br 1H, B–H–Ru), −15.18 (s, 1H, Ru–H–Ru). ^{11}B (C_6D_6): 19.9, 11.3 (1: 2). EIMS: [M^+] 613.1475 (measured), 613.1483 (calculated) for $C_{28}H_{40}B_3Ru_2$. IR (KBr, cm^{-1}): 2492, 2424(ν_{B-H}).

10. NMR ^{1}H(C_6D_6): 7.32 (m, 2H, Ph), 7.24 (m, 3H, Ph), 3.10 (br 1H, B–Ht), 2.78 (m, 2H, CH_2), 2.33 (br 1H, B–Ht), 1.92 (s, 15H, Cp*), 1.83 (s, 15H, Cp*), −2.90 (br 1H, B–H–B), −4.80 (br. 1H, B–H–B), −10.22 (br 1H, B–H–Ru), −11.81 (br 1H, B–H–Ru), −13.40 (br s, 1H, Ru–H(B)–Ru), −13.52 (s, 1H, Ru–H–Ru). ^{11}B(C_6D_6): 9.32, 1.11, −0.72 (1:1:1).

11. NMR ^{1}H (C_6D_6): 7.74 (m, 2H, Ph), 7.47 (m, 2H, Ph), 7.31 (m, 3H, Ph), 7.13 (m, 3H, Ph), 4.60 (br 1H, B–Ht), 4.36 (s, 1H, CH), 3.87 (br 1H, B–Ht), 2.98 (m, 2H, CH_2), 1.36 (m, 2H, CH_2), 1.81 (s, 15H, Cp*), 1.36 (s, 15H, Cp*), −2.35 (br 1H, B–H–B), −10.74 (br 1H, B–H–Ru), −14.66 (s, 1H, Ru–H–Ru), −15.13 (s, br 1H, B–H–Ru). ^{11}B (C_6D_6): 27.95, 24.08, 13.62 (1:1:1). EIMS: [M^+] 720.2372 (measured), 720.2357 (calculated) for $C_{36}H_{51}B_3Ru_2$. IR (KBr, cm^{-1}): 2481, 2436(ν_{B-H}).

12: To **1** (90 mg, 0.17 mmol) in toluene (15 ml) was added PhC ≡ CH (0.2 ml, 1.8 mmol) and the resulting mixture was stirred for 14 h at 60 °C. After removal of solvent and excess alkyne the residue was chromatographed. Elution with hexane–toluene (20:1) gave **9** (14 mg, 13%) and elution with hexane–toluene (10:1) gave **12** (26 mg, 21%) and **11** (34 mg, 28%).

12. NMR ^{1}H (C_6D_6): 7.80–7.05 (m, 10H, Ph), 5.42 (s, 1H, CH), 4.23 (br 1H, B–Ht), 3.87 (br 1H, B–Ht), 2.27 (m, 2H, CH_2), 2.06 (s, 15H, Cp*), 1.59 (s, 15H, Cp*), 0.46 (m, 2H, CH_2), −10.90 (s, br 1H, Ru–H(B)–Ru), −11.42 (s, br 1H, Ru–H(B)–Ru). ^{11}B (C_6D_6): 17.19, 9.69 (1:2). FABMS: 718.2195 (measured), 718.2200 (calculated) for $C_{36}H_{49}B_3Ru_2$. IR (KBr, cm^{-1}): 2482(ν_{B-H}).

4.3. Structure determinations

Crystallographic information for compounds **2**–**6**, **8**, **9** is given in Tables 1 and 2. A suitable crystal, obtained by slow evaporation of a hexane solution at r.t., was placed in inert oil, mounted on a glass pin, and transferred to the cold gas stream of the diffractometer. Crystal data were collected on a Bruker Apex system with graphite monochromated Mo–K_α ($\lambda = 0.71073$ Å)

Table 2
Crystallographic data and structure refinement details for compounds **6**, **8** and **9**

	6	**8**	**9**
Empirical formula	$C_{24}H_{42}B_2Ru_2$	$C_{32}H_{51}BRu_2$	$C_{28}H_{45}B_3Ru_2$
Formula weight	554.34	648.68	616.21
Crystal system	Monoclinic	Triclinic	Monoclinic
Space group	$P2_1/n$	$P\bar{1}$	$P2_1/c$
a (Å)	11.1691(4)	11.1285(4)	11.2796(5)
b (Å)	13.5210(4)	14.8255(6)	14.5579(7)
c (Å)	16.4233(5)	18.4632(7)	17.4134(8)
α (°)	90	94.6200(10)	90
β (°)	96.1010(10)	102.2780(10)	101.6150(10)
γ (°)	90	91.6080(10)	90
V (Å^3)	2466.16(14)	2963.6(2)	2800.9(2)
Z	4	4	4
D_{calc} (g cm^{-3})	1.493	1.454	1.461
$F(000)$	1136	1344	1264
μ (mm^{-1})	1.232	1.037	1.093
Crystal size (mm)	0.3 × 0.25 × 0.2	0.4 × 0.2 × 0.1	0.3 × 0.3 × 0.2
θ Range (°)	1.96–25.00	1.97–28.30	1.84–28.28
Reflections collected	20 014	30 711	30 231
Reflections unique [R_{int}]	4344 [0.0174]	14 451 [0.0186]	6943 [0.0236]
Completeness to θ	$\theta = 25.00$, 100%	$\theta = 28.30$, 98.1%	$\theta = 28.28$, 99.9%
Max. and min. transmission	1.0000, 0.8989	1.0000, 0.8688	1.0000, 0.9140
Refinement method	Full-matrix on F^2	Full-matrix on F^2	Full-matrix on F^2
Data/restraints/parameters	4344/0/251	14 451/0/855	6943/0/301
Goodness-of-fit on F^2	1.064	1.050	1.030
Final R indices [$I > 2\sigma(I)$]	$R_1 = 0.0452$, $wR_2 = 0.1049$	$R_1 = 0.0321$, $wR_2 = 0.0789$	$R_1 = 0.0326$, $wR_2 = 0.0746$
R indices (all data)	$R_1 = 0.0471$, $wR_2 = 0.1064$	$R_1 = 0.0366$, $wR_2 = 0.0817$	$R_1 = 0.0348$, $wR_2 = 0.0761$
Largest difference peak and hole (e Å^{-3})	2.317, −3.054	0.835, −0.687	1.348, −1.268

radiation at 100 K. The structures were solved by direct methods using SHELXS-97 and refined using SHELXL-97 (Sheldrick, G.M., University of Göttingen). Non-hydrogen atoms were found by successive full-matrix least-squares refinement on F^2 and refined with anisotropic thermal parameters. Hydrogen atoms were placed at idealized positions (except Ru–H, B–H hydrogen atoms, which were located from the difference maps). A riding model with fixed thermal parameters [$u_{ij} = 1.2U_{ij\mathrm{eq}}$ for the atom to which they are bonded], was used for subsequent refinements of the hydrogen atoms.

5: Non-hydrogen atoms were found by successive full-matrix least-squares refinement on F^2 and refined with anisotropic thermal parameters, except for disordered Cp* carbon atoms. The asymmetric unit contains two different Ru dimers, and each dimer contains a Cp* ligand which exhibited 2-fold disorder with relative occupancies of 51/49% (one disorder was rotational, the other was a displacement disorder). The disordered carbon atoms were refined isotropically and fixed relative to the rest of the dimer.

6: The internal B_2C_4 moiety was located in two positions as part of a rotational disorder, with 65/35% occupancies. The B–H hydrogen atoms for only the 65% position were located from the difference Fourier maps.

8: The asymmetric unit contains two dimeric units. One of the dimers was found to contain a disorder of the ethyl unit, with relative occupancies of 55 and 45%. The other dimer contained 2-fold rotational disorder in both Cp* units (60/40% occupancies) and the ethyl unit was disordered as well (70/30% disorder).

5. Supplementary material

Crystallographic data for the structures reported in this paper have been deposited with the Cambridge Crystallographic Data Center as supplementary publication no. CCDC no. 180080–180082 for **2**, **6**, **5** and 200817–200820 for **3**, **4**, **8**, **9**. Copies of the data can be obtained free of charge on application to The Director, CCDC, 12 Union Road, Cambridge CB2 1EZ, UK (Fax: +44-1223-336033; e-mail: deposit@ccdc.cam.ac.uk or www: http://www.ccdc.cam.ac.uk).

Acknowledgements

This work was supported by the National Science Foundation CHE 9986880.

References

[1] T.P. Fehlner, J. Chem. Soc. Dalton Trans. (1998) 1525.
[2] T.P. Fehlner, Organometallics 19 (2000) 2643.
[3] H. Hashimoto, M. Shang, T.P. Fehlner, J. Am. Chem. Soc. 118 (1996) 8164.
[4] X. Lei, M. Shang, T.P. Fehlner, J. Am. Chem. Soc. 121 (1999) 1275.
[5] S. Ghosh, X. Lei, C.L. Cahill, T.P. Fehlner, Angew. Chem. Int. Ed. 39 (2000) 2900.
[6] Y. Kawano, H. Matsumoto, M. Shimoi, Chem. Lett. (1999) 489.
[7] L.N. Pangan, Y. Kawano, M. Shimoi, Organometallics 19 (2000) 5575.
[8] L.N. Pangan, Y. Kawano, M. Shimoi, Inorg. Chem. 40 (2001) 1985.
[9] R.N. Grimes, Accts. Chem. Res. 11 (1978) 420.
[10] R.N. Grimes, in: R.N. Grimes (Ed.), Metal Interactions with Boron Clusters, Plenum, New York, 1982, p. 269.
[11] J.D. Kennedy, Prog. Inorg. Chem. 32 (1984) 519.
[12] J.D. Kennedy, Prog. Inorg. Chem. 34 (1986) 211.
[13] C.E. Housecroft, Boranes and Metalloboranes, Ellis Horwood, Chichester, 1990.
[14] G.E. Coates, M.L.H. Green, K. Wade, Organometallic Compounds, third ed., Methuen, London, 1967.
[15] C. Elschenbroich, A. Salzer, Organometallics, VCH, New York, 1989.
[16] R.N. Grimes, Carboranes, Academic Press, New York, 1970.
[17] M.F. Hawthorne, J. Organomet. Chem. 100 (1975) 97.
[18] R.T. Baker, M.S. Delaney, R.E. King, III, C.B. Knobler, J.A. Long, T.B. Marder, T.E. Paxson, R.G. Teller, M.F. Hawthorne, J. Am. Chem. Soc. 106 (1984) 2965.
[19] H. Chen, S. Schlecht, T.C. Semple, J.F. Hartwig, Science 287 (2000) 1995.
[20] C.N. Iverson, M.R. Smith, III, J. Am. Chem. Soc. 121 (1999) 7696.
[21] R.N. Grimes, Pure Appl. Chem. 39 (1974) 455.
[22] R. Weiss, J.R. Bowser, R.N. Grimes, Inorg. Chem. 17 (1978) 1522.
[23] E.J. Ditzel, X.L.R. Fontaine, N.N. Greenwood, J.D. Kennedy, Z. Sisan, B. Stibr, M. Thornton-Pett, J. Chem. Soc. Chem. Commun. (1990) 1741.
[24] J. Bould, N.P. Rath, L. Barton, Organometallics 15 (1996) 4916.
[25] J. Bould, N.P. Rath, L. Barton, J.D. Kennedy, Organometallics 17 (1998) 902.
[26] H. Yan, A.M. Beatty, T.P. Fehlner, Angew. Chem. Int. Ed. 40 (2001) 4498.
[27] H. Yan, A.M. Beatty, T.P. Fehlner, Angew. Chem. Int. Ed. 41 (2002) 2578.
[28] H. Yan, A.M. Beatty, T.P. Fehlner, J. Am. Chem. Soc. 124 (2002) 10280.
[29] K. Wade, Adv. Inorg. Chem. Radiochem. 18 (1976) 1.
[30] D.M.P. Mingos, D.J. Wales, Introduction to Cluster Chemistry, Prentice Hall, New York, 1990.
[31] P. McQuade, K. Hupp, J. Bould, H. Fang, N.P. Rath, R.L. Thomas, L. Barton, Inorg. Chem. 38 (1999) 5415.
[32] O. Hollander, W.R. Clayton, S.G. Shore, Chem. Commun. (1974) 604.
[33] H. Braunschweig, C. Kollann, U. Englert, Eur. J. Inorg. Chem. (1998) 465.
[34] J.C. Calebrese, M.B. Fischer, D.F. Gaines, J.W. Lott, J. Am. Chem. Soc. 96 (1974) 6318.
[35] G.M. Dawkins, M. Green, A.G. Orpen, F.G.A. Stone, J. Chem. Soc. Chem. Commun. (1982) 41.
[36] K. Knoll, G. Huttner, L. Zsolnai, I. Jibril, M. Wasincionek, J. Organomet. Chem. 294 (1985) 91.
[37] S.G. Shore, in: E.L. Muetterties (Ed.), Boron Hydride Chemistry, Academic Press, New York, 1975, p. 79.
[38] D.F. Gaines, Accts. Chem. Res. 6 (1973) 416.
[39] S. Ghosh, X. Lei, M. Shang, T.P. Fehlner, Inorg. Chem. 39 (2000) 5373.

[40] H.C. Brown, Hydroboration, Benjamin, New York, 1962.
[41] R. Wilczynski, L.G. Sneddon, Inorg. Chem. 20 (1981) 3955.
[42] H. Brumberger, R.A. Marcus, J. Chem. Phys. 24 (1956) 741.
[43] R.E. Williams, Prog. Boron Chem. 2 (1970) 37.
[44] M.A. Cavanaugh, T.P. Fehlner, R. Stramel, M.E. O'Neill, K. Wade, Polyhedron 4 (1985) 687.
[45] H. Yan, A.M. Beatty, T.P. Fehlner, Organometallics 21 (2002) 5029.
[46] J.R. Morrey, A.B. Johnson, Y.-C. Fu, G.R. Hill, Adv. Chem. Ser. 32 (1961) 157.
[47] T.L. Venable, R.N. Grimes, Inorg. Chem. 21 (1982) 887.
[48] B.H. Goodreau, L.R. Orlando, J.T. Spencer, Inorg. Chem. 31 (1992) 1731.
[49] C.N. Iverson, M.R. Smith, III, Organometallics 15 (1996) 5155.
[50] T. Sagawa, Y. Asano, F. Ozawa, Organometallics 21 (2002) 5879.
[51] G.E. Herberich, in: E. Abel, F.G.A. Stone, G. Wilkinson (Eds.), Comprehensive Organometallic Chemistry II, vol. 1, Pergamon Press, Oxford, 1995, p. 197.
[52] M. Herberhold, H. Yan, W. Milius, B. Wrackmeyer, Angew. Chem. Int. Ed. 38 (1999) 3689.
[53] M. Herberhold, H. Yan, W. Milius, B. Wrackmeyer, J. Chem. Soc. Dalton (2001) 1782.
[54] D.F. Shriver, M.A. Drezdzon, The Manipulation of Air Sensitive Compounds, second ed., Wiley-Interscience, New York, 1986.